Environmental Research Letters

ACCEPTED MANUSCRIPT • OPEN ACCESS

Spatial mapping of short-term solar radiation prediction incorporating geostationary satellite images coupled with deep convolutional LSTM networks for South Korea

To cite this article before publication: Jong-Min Yeom *et al* 2020 *Environ. Res. Lett.* in press https://doi.org/10.1088/1748-9326/ab9467

Spatial mapping of short-term solar radiation prediction incorporating geostationary satellite images coupled with deep convolutional LSTM networks for South Korea

Jong-Min Yeom[1] Ravinesh C Deo[2], Jan F Adamowski[3], Seonyoung Park[1], Chang-Suk Lee[4]*

[1] Satellite Application Division, Korea Aerospace Research Institute, 115 Gwahangno, Yuseong-gu, Daejeon, 34133, REPUBLIC OF KOREA

[2] School of Sciences, Centre for Sustainable Agricultural Systems & Centre for Applied Climate Sciences, University of Southern Queensland, QLD 4300, AUSTRALIA

[3] Department of Bioresource Engineering, Faculty of Agricultural and Environmental Sciences, McGill University, Montreal, CANADA

[4] National Institute of Environmental Research, 42, Hwangyong-ro, Seogu, Incheon, 22689, REPUBLIC OF KOREA

E-mail: leecs00@korea.kr

Received
Accepted for publication
Published

Abstract

A practical approach to continuously monitor and provide real-time solar energy prediction can help support reliable renewable energy supply and relevant energy security systems. In this study on the Korean Peninsula, contemporaneous solar radiation images obtained from the Communication, Ocean and Meteorological Satellite (COMS) Meteorological Imager (MI) system, were used to design a convolutional neural network and a long short-term memory network predictive model, ConvLSTM. This model was applied to predict one-hour ahead solar radiation and spatially map solar energy potential. The newly designed ConvLSTM model enabled reliable prediction of solar radiation, incorporating spatial changes in atmospheric conditions and capturing the temporal sequence-to-sequence variations that are likely to influence solar driven power supply

and its overall stability. Results showed that the proposed ConvLSTM model successfully captured cloud-induced variations in ground level solar radiation when compared with reference images from a physical model. A comparison with ground pyranometer measurements indicated that the short-term prediction of global solar radiation by the proposed ConvLSTM had the highest accuracy [root mean square error (RMSE) = 83.458 $W \cdot m^{-2}$, mean bias error (MBE) = 4.466 $W \cdot m^{-2}$, coefficient of determination (R^2) = 0.874] when compared with results of conventional artificial neural network (ANN) [RMSE = 94.085 $W \cdot m^{-2}$, MBE = −6.039 $W \cdot m^{-2}$, R^2 = 0.821] and random forest (RF) [RMSE = 95.262 $W \cdot m^{-2}$, MBE = −11.576 $W \cdot m^{-2}$, R^2 = 0.839] models. In addition, ConvLSTM better captured the temporal variations in predicted solar radiation, mainly due to cloud attenuation effects when compared with two selected ground stations. The study showed that contemporaneous satellite images over short-term or near real-time intervals can successfully support solar energy exploration in areas without continuous environmental monitoring systems, where satellite footprints are available to model and monitor solar energy management systems supporting real-life power grid systems.

Keywords: Solar radiation prediction, convolutional neural network, long short-term memory, COMS-MI, pyranometer, deep learning

1. Introduction

Successful integration of the rapidly growing renewable energy production into existing or future power grid systems is an important challenge for the future global energy supply. Any electricity operator needs to ensure a precise balance between electricity production and consumption to reduce overall costs and sustain electricity production [1]. Existing energy plants that run on nuclear power, steam (thermal resources), fossil fuels (coal), and hydropower can control their energy production according to expected consumption by responding to the different temporal horizons of their operational power systems [2]. However, solar energy is intermittent and unpredictable due to its high sensitivity to atmospheric conditions. It is also generated by spatially dispersed, small scale power plants [3, 4]. This adds to the risk or uncertainty underlying system management, which in turn increases the cost of solar power production.

New approaches are required to predict the spatiotemporal distribution of solar radiation with a reliable degree of accuracy. These will optimize the integration of solar energy into existing electrical power grids and ensure its favorable trading performance and sustainability in the modern electricity market [5].

Numerical Weather Prediction (NWP) models are the 'gold standard' for building frameworks based on mathematical equations that seek to emulate changes in global solar radiation [6]. The main advantage of such models is their dynamical modelling ability to represent atmospheric properties. For example, solar radiation is predicted by interpreting physical processes of atmospheric flows, as well as by considering cloud movement and other atmospheric components. Real-time solar energy power generating systems require short-term predictions (within 6h). However, NWP models are relatively less reliable for short-term prediction of solar radiation because the models need to derive a physical valid state after initialization (called the spin-up time). In particular, very short-term forecasts (nowcast) of 1–2 h ahead, derived by NWP, are less accurate than those provided by Machine Learning (ML) approaches [7, 8].

ML algorithms including artificial neural network (ANN), support vector machine (SVM), and random forest (RF) are recently developed alternatives to NWP models and have been widely applied to predict global solar radiation [9–16]. Many of these new models use atmospheric datasets of a sufficient length and quality as well as relevant parameters to explain the variations in solar radiation over a historical period. ML approaches have attained a high degree of accuracy in the retrieval and prediction of global solar radiation at the Earth's surface [17–22]. The main advantage of ML models, as compared with the NWP model, is that the former can simulate the spatiotemporal characteristics of global solar radiation simply by using ground pyranometer or satellite datasets, without understanding the complicated physical processes or the related solar radiation dynamics. However, existing ML models are unable to consider environmental

information beyond the target points [23, 24]. As solar radiation varies in time and space due to the effects of cloud movements and the components of the atmosphere [25], existing ML methods based on shallow network structures (less than two layers), and fixed initial conditions [26, 27] are limited with regard to the prediction of spatiotemporal solar radiation.

Deep learning models such as deep neural networks (DNNs), long short-term memory (LSTM) networks, and convolutional neural network algorithms, have been developed to solve complex and nonlinear problems in the fields of computer vision and remote sensing [1, 31–34], and more recently, solar energy prediction [28-30]. These newer methods allow for the building of deeper, more complex network structures (often based on multiple hidden layers in the overall model architecture) to accurately identify the key features present in the predictor(s) and target variables [32]. Implementing multiple hidden layers can avoid vanishing gradient descents and over-fitting issues, which are typical in single hidden layer ML models. New activation functions such as a rectified linear unit (ReLU) have led to a better dropout rate and more effective initialization of kernels or weights. Deep learning algorithms can generate accurate predictions, particularly for relatively complex and stochastic datasets [35–37].

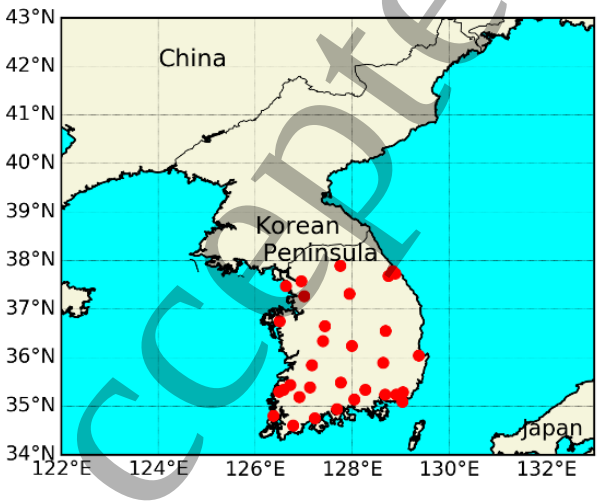

Figure 1. Map of the study area and locations of ground pyranometers (red dots) using World Geodetic System (WGS) 84 geographic projection.

Considering the potential benefits of deep learning-based models, the aims of this study were to: (*i*) develop a new convolutional long short-term memory (ConvLSTM) model for one-hour ahead solar radiation prediction using geostationary contemporaneous satellite images, and (*ii*) generate spatial solar radiation maps of the Korean Peninsula using the ConvLSTM model. The novelty of this study is the newly designed ConvLSTM model that integrates continuous COMS-MI images to provide spatiotemporal variations in solar radiation at any specific point.

2 Materials and Methods

2.1. Study area and satellite imagery for training the deep learning model

The study area covers the Korean Peninsula (Figure 1). It has a temperate monsoon climate, with a cold continental climate in the north (similar to northern China) and a marine climate in the south (similar to southern Japan [38]). The 33 ground pyranometers (model CM21, Kip & Zonen) operated by the Korea Meteorological Administration (red dots in Figure 1) provided ground

measurements of solar radiation with hourly resolution (available at https://data.kma.go.kr). The quality control procedures followed the criteria of the Guide to Meteorological Instruments and Methods of Observation World Meteorological Organization (WMO) No. 8. These measurements served to validate global solar radiation predictions generated by the deep learning-based ConvLSTM model and conventional ANN and RF models. In the present study, the COMS-MI satellite was mainly used to estimate spatiotemporal solar radiation as an input parameter [39]. COMS-MI has five spectral bands, ranging from visible to infrared, with spatial resolutions of 1–4 km. These bands have proved to be quite useful in observing atmospheric conditions such as cloud cover and atmospheric gas concentrations. The temporal resolution of the COMS-MI device ranges from about 15 min to 3 h depending on where the observation is made [40]. Therefore, it is possible to make a time series of global solar radiation images to reflect the continuous flow of the atmosphere. In this study, the global solar radiation was first estimated by a physical model that used COMS-MI satellite spectral bands and atmospheric information. Subsequently, the same time series of solar radiation only served as the input data for the DNN, ANN, and RF models to reduce the size of the computation memory [41-43]. For more details of the physical model's development, readers may consult previous studies [43, 44].

Our estimation of hourly global solar radiation using a physical model employed COMS-MI dataset collected from a total of 1,100 sequential images between April 1, 2011 and December 31, 2015 (parts of the time series data were not available due to a change in observation mode). These data, consecutively recorded between 09:00 h and 13:00 h local time, were required to predict daytime solar radiation at 14:00 h (*i.e.*, at least 1 h after the observation). The main reasons for predicting one hour ahead solar radiation is that short-term prediction is useful for determining whether or not the existing power generation is operating [1]. To construct the deep learning-based ConvLSTM and conventional ANN and RF models, the full dataset was divided into three distinct parts in chronological order: training, validation, and test datasets. 80% of the total datasets were used for training and validation of the data-driven models from April 1, 2011 to September 8, 2015 (880 images). Among this 80%, about 10% (i.e., 110 images) was used for validation of the ML models during the training process to reduce over-fitting problems. The remaining 20% from September 9, 2015 to December 31, 2015 (220 images) was used to test the ML models to evaluate the performance and generalization of these models.

2.2. Framework of the ConvLSTM DNN model

The DNN algorithm employed in the present study is considered to be an LSTM model, a variant of the recurrent neural network (RNN) algorithm. The RNN algorithm suffers from a drawback: a complex neuronal structure can result in a "vanishing gradient," which can make long-term predictions relatively difficult [44, 46].

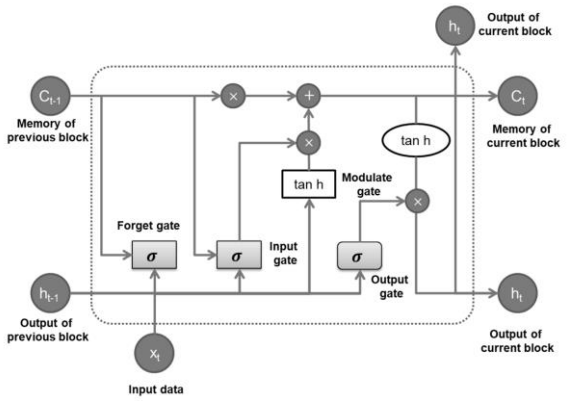

Figure 2 Schematic of the long short-term memory (LSTM) algorithm used to predict solar radiation.

To overcome this issue, the present study implemented the LSTM algorithm (Figure 2), which introduced a memory block instead of a neuron [47, 48].

According to Shi et al. [49], LSTMs and ConvLSTM (which uses a convolutional system) have identical basic structures, but the more advanced ConvLSTM algorithm uses a three-dimensional (3D) tensor for all gates and relevant input/output variables. Furthermore, all the matrix calculations are changed according to the convolutional process, such that the number of weightings and biases are dramatically reduced. These changes can allow the ConvLSTM algorithm to successfully capture spatial features and temporal features in the model's input data. In this study, we used the ConvLSTM algorithm with a Tensorflow backend, available from the Keras library of Python software version 3.6.

To configure the most suitable ConvLSTM model structure, this study employed techniques previously used for video frame predictions [50] as well as short-term rainfall predictions [51]. The basic structure of the suggested model consists of a combination of hidden layers1 (stacked ConvLSTM2D layers) and hidden layers2 (stacked Conv3D, ConvLSTM2D, Conv2D layers) sections (Figure 3). In hidden layers1, the spatiotemporal features of the continuous solar radiation from 09:00 to 13:00 are captured, and the spatiotemporal features stretched by time are compressed into a target time (14:00) in hidden layers2.

Between all convolution layers, a batch normalization layer was inserted to increase the training speed and prevent over-fitting [52]. These convolution layers used 40 filters, the "ReLU" activation function and the "He normal" initializer, except for Conv2D (single filter). The initializer of the filter weights prevented the gradient vanishing problem during back-propagation of the error and improved the predictive performance [53, 54]. The "ReLU" activation function is widely used for training procedures, and application of the "He normal" initializer is suitable for "ReLU" activation [53]. In the fitting process, the mean squared error (MSE) loss function coupled with the Adam optimizer was implemented because the target variable (solar radiation) is a floating number with a physical unit ($W \cdot m^{-2}$). To identify the optimal structure of the ConvLSTM model for predicting global solar radiation, the number of ConvLSTM2D layers was varied within a range of 1 to 4 (Hidden Layers1, Figure 3).

In addition, we compared the conventional data-derived models, ANN and RF [55, 56], with the performance of the proposed DNN model.

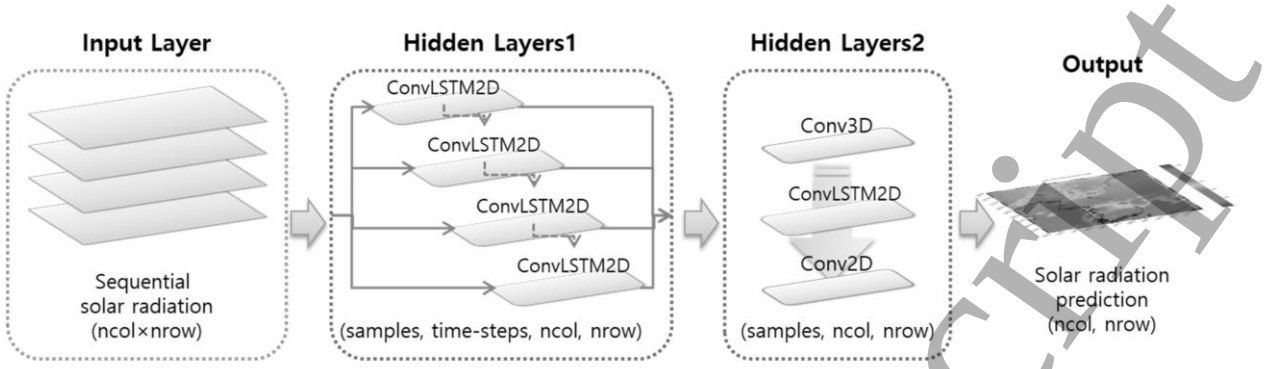

Figure 3. Prototype structure for training the deep learning model to predict solar radiation.

In the case of ANN, we designed the neural network structure with three layers, namely the input, hidden, and output layers [55]. One hidden layer has several hidden nodes, including the activation function and weights. To avoid over-fitting to the training data, we adopted early stopping during the training process. A trial and error method was used to determine the number of optimal nodes in the hidden layer. RF is a combination of several decision trees (30 trees in this study) with randomized node optimization and bootstrap aggregating [14, 56, 57]. To enhance the generality and prediction performance of the trained RF model, we set the ratio of the amount of data and the number of input variables to be used in each tree. We tested the combination of the number of input variables (2 and 3) and the ratio of the amount of input data (0.5, 0.632, and 0.8), and found the optimum configuration to be 2 variables with an input ratio of 0.8 [58].

3 Results and Discussion

3.1. Evaluation of the ConvLSTM model performance

We used the root mean square error (RMSE) between the observed and predicted values of solar radiation to assess the accuracy of four different ConvLSTM models and found relatively small differences (Table 1). The three-layer ConvLSTM2D algorithm used the lowest number of training epochs and proved to be the most accurate (see Figure S1 (c) in the supplementary file). In contrast, the two-layer ConvLSTM model had the highest number of training epochs and the lowest accuracy, and the learning process changed due to the unstable loss of the evaluation data (see Figure S1 (b) in the supplementary file). The most complicated model, the four-layer ConvLSTM2D, required the second highest number of epochs. The single layer ConvLSTM model showed an unstable trend of validation loss and relatively low accuracy. These results indicated that the simple structure model was limited in terms of accuracy improvement, but that problems such as over-fitting also occurred in the complex model. Based on this analysis, we selected the three-layer ConvLSTM

Table 1. Summary of the prediction results according to the structures of the tested ConvLSTM models

Model structure (kernel size)	Number of parameters	MSE (RMSE) ($W \cdot m^{-2}$)	Epochs
ConvLSTM2D(3×3) 1 layer-Conv3D(3×3×3)-ConvLSTM2D(3×3)-Conv2D(1×1)	218,321	*5757.25 (75.88)*	*69*
ConvLSTM2D(3×3) 2 layer-Conv3D(3×3×3)-ConvLSTM2D(3×3)-Conv2D(1×1)	333,841	*6010.87 (77.92)*	*80*
ConvLSTM2D(3×3) 3 layer-Conv3D(3×3×3)-ConvLSTM2D(3×3)-Conv2D(1×1)	449,361	*4981.41 (70.58)*	*59*
ConvLSTM2D(3×3) 4 layer-Conv3D(3×3×3)-ConvLSTM2D(3×3)-Conv2D(1×1)	564,881	*5545.96 (74.47)*	*77*

model and applied it to predict global solar radiation one hour after the input data were measured.

3.2. Evaluation of predicted solar radiation maps using the three-layer ConvLSTM model

Global solar radiation maps generated from values predicted for the Korean Peninsula served to visually evaluate the performance of the proposed ConvLSTM model with only the test datasets. The results of the ANN and RF models were compared against those of the proposed ConvLSTM. Figure 4 shows three examples of predicted global solar radiation maps acquired from the ANN, RF and three-layer ConvLSTM models as well as the physically based model. Overall, the spatial patterns of solar radiation for all three selected samples were well predicted using the ANN, RF, and ConvLSTM models compared with the corresponding maps generated from the output of the physical model (Figure 4 (a), (e), and (i)). For the ConvLSTM model, the complex spatial patterns of clouds, which lower the solar radiation incident on the Earth's surface, were well simulated using the proposed deep learning approach. The high attenuation areas due to the prevalence of thick cloud (shown in dark blue) and the spatial location of the surrounding thin clouds (shown in sky blue) were well matched. However, although the spatial location and shapes of the clouds appeared to be in good agreement, the predicted maps of global solar radiation were relatively smooth in comparison with those derived from the physical model and conventional ML methods. This was predominantly attributed to the convolutional filter of the DNN structure.

For the conventional ANN and RF models, the predicted maps of solar radiation were similar. These models predicted one hour ahead solar radiation by training or validating their network weights based on the difference of each pixel, unlike the convolutional filter. Therefore, they predicted more detailed spatial patterns of clouds and intensities of high and low values of solar radiation than the ConvLSTM model. Nevertheless, some problems persisted with the ANN and RF models. In the first and second rows in Figure 4, the red circled areas contain thin clouds (Figures 4 (b), (c), and (f), (g)) that do not exist in the reference images (a), and (e); thus, the clouds were predicted incorrectly by both models. This could be caused by a biased training towards clear and thick cloud cases that have more examples and are easier to predict

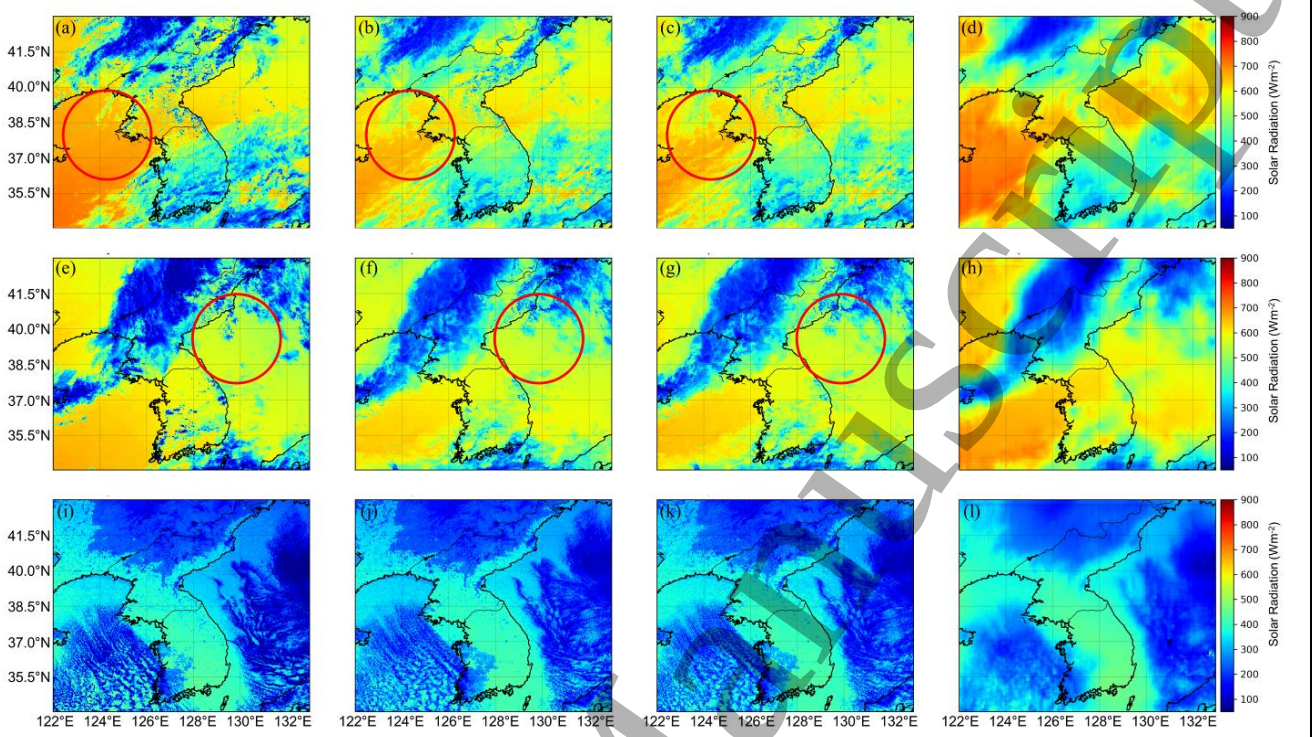

Figure 4. Predicted global solar radiation maps for the Korean Peninsula developed using the ANN, RF, proposed ConvLSTM, and the physical models for 14:00 h (local time) September 25, 2015, 14:00 h (local time) October 8, 2015, and 14:00 h (local time) December 17, 2015. The red circles represent areas that are incorrectly predicted to be cloudy in the ANN and RF models.

than thin clouds since the optimizing process of the ML models was designed to increase the total accuracy. In addition, the prediction of global solar radiation by the ANN and RF models appeared to be underestimated when compared with the ConvLSTM and physical models.

We used two reference datasets to appraise the performance of our data-driven model: reference images from the physical model and ground measurements from the pyranometers located in South Korea. First, each of the predicted solar radiation maps from the data-driven models was validated with reference images of the physical model using only the test datasets (from September 9, 2015 to December 31, 2015), as shown in the density scatter plots in Figure 5. All the data-driven approaches showed good predictions of one-hour ahead solar radiation using their own trained network structures integrated with the COMS geostationary satellite data. For all three cases, the highest density in each figure appeared in an area that received a low level of solar radiation, which was attributed to cloud effects. Among the data-driven models, the predictions of the ConvLSTM model in Figure 5 (a) showed the highest statistical agreement (RMSE = 71.334 W·m^{-2}, R^2 = 0.895) with the reference images of the test dataset. However, the MBE of ConvLSTM was higher, which indicated it tended to overestimate more than the other models. Nevertheless, the Inter-Quartile Range (IQR) distribution of ConvLSTM was narrower, and the range of the overall deviation was

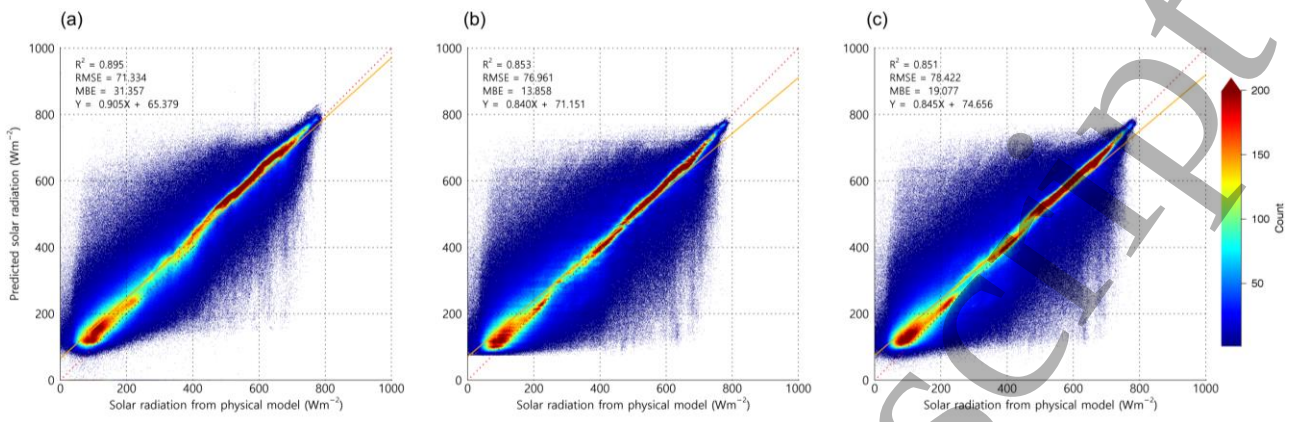

Figure 5. Density scatterplots describing the correlation between the reference images from the physical model and the predicted maps of solar radiation data for the test dataset only. Performance of each data-driven model was validated using the reference images of the physical model. Results for (a) ConvLSTM, (b) RF, and (c) ANN models. The dotted line is the one-to-one reference line, and the solid line is the regression line.

smaller compared to the ANN and RF models (see Figure S2 in supplementary file). Extreme values tended to be reduced by considering the spatial relation of neighboring pixels with the convolutional filer. The second and third highest accuracies were obtained by the RF (RMSE = 76.961 W·m^{-2}, R^2 = 0.853) and ANN (RMSE = 78.422 W·m^{-2}, R^2 = 0.851) models (Figure 5 (b) and (c), respectively), but these results were not significantly different from those of the proposed deep learning approach.

Second, the predicted solar radiation data from each model were compared with those recorded at the ground stations scattered across South Korea to calculate the actual amount of solar energy available to the photovoltaic (PV) systems. Ground-based pyranometers were considered the ultimate reference for validating the solar radiation predicted by the models. However, unlike the reference images from the test dataset, a test on the pyranometer measurements of solar radiation through satellite observations was performed. This determined the spatial representativeness of the ground stations due to spatial discrepancies induced by the systematic differences between pixel-based satellite global solar radiation and hemisphere upward-looking-based pyranometer measurements [44]. For the ConvLSTM model, the predicted solar radiation showed the highest correlation with the ground measurements under all sky conditions (Figure 6a) and also showed the highest accuracy (RMSE = 83.458 W·m^{-2}, MBE = 4.466 W·m^{-2}, coefficient of determination (R^2) = 0.874) with the ground pyranometer data when compared with the conventional ML methods. In addition, the prediction accuracy of the solar radiation by ConvLSTM was comparable and almost similar to the retrieval accuracy of the physical model (RMSE = 81.843 W·m^{-2}, MBE = 8.414 W·m^{-2}, R^2 = 0.880; see Figure S3 in the supplementary file). The ANN (RMSE = 94.085 W·m^{-2}, MBE = -6.039 W·m^{-2}, R^2 = 0.821) and RF (RMSE

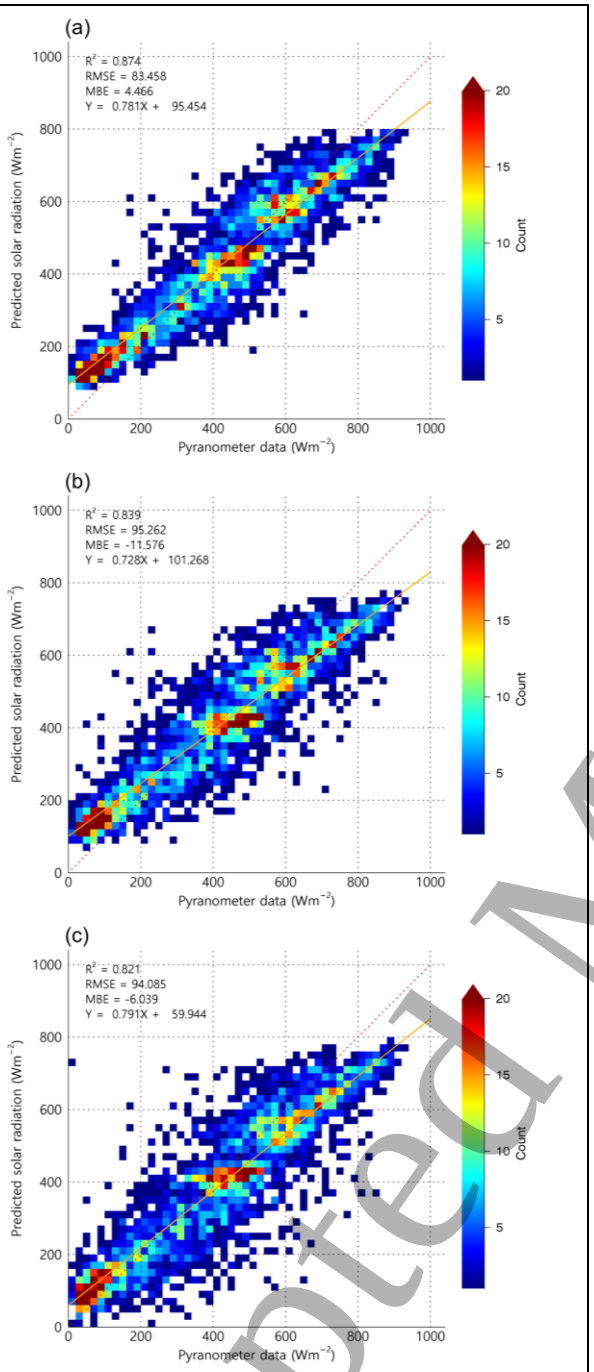

Figure 6. Density scatterplots describing the correlation between ground pyranometer data and modeled solar radiation data. Model results from the (a) ConvLSTM, (b) RF, and (c) ANN models were validated with pyranometer measurements located on the ground in South Korea.

= 95.262 W·m^{-2}, MBE = -11.576 W·m^{-2}, R^2 = 0.839) models were less accurate (Figures 6 (c) and (b), respectively). Results indicated that the existing ML methods somewhat underestimated the values compared to the ground measurements. This is consistent with the statistical results of the ConvLSTM prediction maps that were compared with the reference images of the physical model in Figure 5. In addition, the accuracy of the statistical results is different from that of the reference images and ground measurements used to validate the data-driven models (Figures 5 and 6). This is because of the difference between pixel-to-pixel comparisons for reference images and the manner of determining which window of the satellite corresponded to which ground measurement stations. In other words, when compared with ground measurements, spatial window size around the station was more important than the pixel value corresponding to the position of the ground measurement due to the hemisphere upward-looking-based pyranometer measurements. This may have resulted in the higher accuracy of ConvLSTM when compared with ground pyranometer data because convolutional filters of DNN were able to train environmental information beyond the target points, ensuring successful capture of the spatial features of solar radiation.

The proposed ConvLSTM algorithm has been proven to effectively simulate the variations in solar radiation under all sky conditions using the test dataset from late summer to early winter. Since the influence of clouds is the largest factor in determining the accuracy of solar radiation, ConvLSTM would also be applicable to the whole year [14, 43, 59].

Lastly, we analyzed the temporal changes in the predicted solar radiation from each model to determine how well the

proposed methods captured the abnormal variations in solar radiation due to cloud effects. Figure 7 shows time series comparisons of the solar radiation on each day from DNN, RF, and ANN using the ground pyranometer, predicted one-hour ahead (at 14:00 local time) from the chronological test dataset. We selected two stations ((a) Heuksando, (b) Jeonju)), which had the largest standard deviation during the test dataset periods. The overall trends in time series of solar radiation were decreasing during the winter season for both sites, and intermittent low peak values were mainly due to the attenuation by cloud effects. ConvLSTM (red long dash lines) not only captured the dramatic decreases in solar radiation well (Figure 7), but also clearly had the highest accuracies for Heuksando (RMSE=77.445 $W \cdot m^{-2}$, MBE= -11.707 $W \cdot m^{-2}$) and Jeonju (RMSE=81.890 $W \cdot m^{-2}$, MBE= -28.378 $W \cdot m^{-2}$). However, besides cloud effects, there are some atmospheric factors that may rapidly reduce solar radiation such as fire haze, smog, and particulate matter. Although it is difficult to evaluate the influences on solar radiation by various atmospheric variables using COMS satellites and pyranometers only, we believe that the prediction algorithms presented in this study are useful in developing predictions model for more diverse atmospheric variables using appropriate satellite and ground sensors.

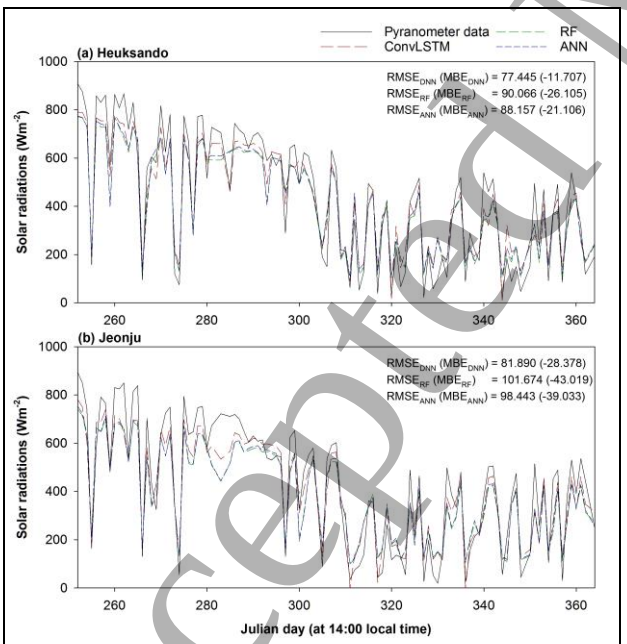

Figure 7. Time series comparisons of solar radiations from each of DNN (red long dash line), RF (green medium dash line), ANN (blue short dash line) with ground pyranometer (black line) for the test dataset at every 14:00 local time. The two of ground stations for Heuksando (a), and Jeonju (b) were selected based on the scale of solar radiation variations.

Summary and Conclusions

The DNN algorithm (*i.e.*, ConvLSTM) proposed in this paper can produce reliable simulations with fewer variables, but the depth of such a model network structure is not directly proportional to the accuracy of the predictions. To improve the versatility of the ConvLSTM model, this study examined four different DNN structures, each with a different depth, to construct the optimal number of ConvLSTM2D layers. To avoid over-fitting and gradient vanishing, we used several built-in model optimization options, such as batch normalization, initialization of kernel weights and an early stopping phase. The three-layer ConvLSTMD algorithm was found to be optimal and was used to generate spatial maps of solar radiation. Results were compared against those of the physical model as well as conventional ML methods.

Overall, the results showed that the ConvLSTM model was able to predict maps of solar radiation relatively well, even in the presence of nonlinearities (*e.g.*, cloud movements), which are inherent in any dynamical system. In particular, the spatial patterns representing complex cloud movements and their dynamical intensities (including attenuations) were spatially well matched against maps derived from a physical model. The accuracy of the ConvLSTM model prediction maps had the highest agreement with both the reference images of the physical model and the ground reference data compared to the results of the ANN and RF approaches. For the reference images, ConvLSTM showed the highest accuracy (RMSE = 71.334 $W \cdot m^{-2}$, R^2 = 0.895), followed by RF and ANN (RMSE = 76.961 $W \cdot m^{-2}$, R^2 = 0.853; and RMSE = 78.422 $W \cdot m^{-2}$, R^2 = 0.851, respectively). Compared to the ground pyranometer data, ConvLSTM also showed the highest accuracy (RMSE = 83.458 $W \cdot m^{-2}$ and MBE = 4.466 $W \cdot m^{-2}$, R^2 = 0.874) compared to the ANN (RMSE = 94.085 $W \cdot m^{-2}$, MBE = −6.039 $W \cdot m^{-2}$, R^2 = 0.821) and RF (RMSE = 95.262 $W \cdot m^{-2}$, MBE = -11.576 $W \cdot m^{-2}$, R^2 = 0.839) methods. Although the spatially representative solar radiation maps became relatively smooth due to the convolutional filters, the ConvLSTM model was useful to capture the spatial features of solar radiation according to atmospheric flow. In addition, calculation time is also an important factor for the real-time application of prediction models. In the case of DNN, the prediction took 0.042 seconds per image (see Table S1 in supplementary file), indicating that the calculation speed was appropriate. Thus, this study highlights a new pathway for using contemporaneous satellite images to capture the nonlinear behavior of the atmospheric system to design and manage solar-powered energy systems.

Acknowledgments

We are grateful to the editors and anonymous referees for their helpful comments and suggestions. This work was supported by a grant from the National Institute of Environmental Research (NIER), funded by the Ministry of Environment (MOE) of the Republic of Korea (NIER-2019-01-01-027) and the Korea Aerospace Research Institute (FR20G00).

Data availability statement

The data that support the findings of this study are available from the corresponding author upon reasonable request.

References

[1] Voyant C, Notton G, Kalogirou S, Nivet M L, Paoli C, Motte F and Fouilloy A 2017 Machine learning methods for solar radiation forecasting: A review. *Appl. Energy*. **105** 569

[2] Liu Y, Qin H, Zhang Z, Pei S, Wang C, Yu X, Jiang Z, and Zhou J 2019 Ensemble spatiotemporal forecasting of solar irradiance using variational Bayesian convolutional gate recurrent unit network. *Appl. Energy*. **253** 113596

[3] Fouilloy A, Voyant C, Notton G, Motte F, Paoli C, Nivet

M L, Guillot E, and Duchaud J L 2018 Solar irradiance prediction with machine learning: Forecasting models selection method depending on weather variability. *Energy* **165(15)** 620

[4] Lou S, Li D H W, Lam JC and Chan W W H 2016 Prediction of diffuse solar irradiance using machine learning and multivariable regression. *Appl Energy*. **181** 367

[5] Martín L, Zarzalejoso L F, Polo J, Navarro A, Marchante R and Cony M 2010 Prediction of global solar irradiance based on time series analysis: application to solar thermal power plants energy production planning. *Sol. Energy*. **84** 1772

[6] Perez R, Lorenz E, Pelland S, Beauharnois M, Knowe G V, Hemker Jr. K, Heinemann D, Remund J, Müller SC, Traunmüller W and Steinmauer G 2013 Comparison of numerical weather prediction solar irradiance forecasts in the US, Canada and Europe. *Sol. Energy*. **94** 305

[7] Sun J 2014 Use of NWP for nowcasting convective precipitation: recent progress and challenges. *Bull. Am. Meteor. Soc*. 409

[8] Inman R H, Pedro H T C and Coimbra C F M 2013 Solar forecasting methods for renewable energy integration. *Prog. Energ. Combust. Sci.* **39** 535

[9] Deo R C, Wen X and Qi F 2016 A wavelet-coupled support vector machine model for forecasting global incident solar radiation using limited meteorological dataset. *Appl. Energy*. **168** 568

[10] Salcedo-Sanz S, Deo R C, Cornejo-Bueno L, Camacho-Gómez C and Ghimire S 2018 An efficient neuro-evolutionary hybrid modelling mechanism for the estimation of daily global solar radiation in the Sunshine State of Australia. *Appl. Energy*. **209** 79

[11] Ghimire S, Deo R C, Raj N and Mi J 2019 Wavelet-based 3-phase hybrid SVR model trained with satellite-derived predictors, particle swarm optimization and maximum overlap discrete wavelet transform for solar radiation prediction. *Renew. Sustain. Energy Rev.* **113** 109247

[12] Behrang M A, Assareh E, Ghanbarzadeh A and Noghrehabadi A R 2010 The potential of different artificial neural network (ANN) techniques in daily global solar radiation modeling based on meteorological data. *Sol. Energy*. **84** 1468

[13] Huang J, Troccoli A and Coppin P 2014 An analytical comparison of four approaches to modelling the daily variability of solar irradiance using meteorological records. *Renew. Energy*. **72** 195

[14] Yeom J M, Park S, Chae T, Kim J Y and Lee C S 2019 Spatial assessment of solar radiation by machine learning and deep neural network models using data provided by the COMS MI geostationary satellite: A case study in South Korea. *Sensors*. **19** 2082

[15] Wang, L Kisi O, Zounemat-Kermani M, Salazar G A Zhu Z and Gong W 2016 Solar radiation prediction using different techniques: model evaluation and comparison. *Renew. Sustain. Energy Rev*. **61** 384

[16] Zou L, Wang L, Xia L, Lin A, Hu B and Zhu H 2017 Prediction and comparison of solar radiation using improved empirical models and Adaptive Neuro-Fuzzy Inference systems. *Renew. Energy*. ***106*** *343*

[17] Fadare D A 2009 Modelling of solar energy potential in Nigeria using an artificial neural network model. *Appl. Energy*. **86(9)** 1410

[18] McCulloch W S and Pitts W 1943 A logical calculus of the ideas immanent in nervous activity. *Bull. Math. Biophys*. **5** 115

[19] Keshtegar B, Mert C and Kisi O 2018 Comparison of four heuristic regression techniques in solar radiation modeling: Kriging method vs RSM, MARS and M5 model tree. *Renew. Sustain. Energy Rev*. **81** 330

[20] Qin W, Wang L, Lin A, Zhang M, Xia X, Hu B and Niu Z 2018 Comparison of deterministic and data-driven models for solar radiation estimation in China. *Renew. Sust. Energy Rev.* **81** 579

[21] Deo R C and Sahin M 2017 Forecasting long-term global solar radiation with an ANN algorithm coupled with satellite-derived (MODIS) land surface temperature (LST) for regional locations in Queensland. *Renew. Sustain. Energy Rev.* **72** 828

[22] Qin W., Wang L, Zhang M and Niu Z 2019 First effort at constructing a high-density photosynthetically active radiation dataset during 1961-2014 in China. *J. Climate.* **32** 2761

[23] Ndikumana E, Ho T M D, Baghdadi N, Courault D and Hossard L 2018 Deep recurrent neural network for agricultural classification using multi temporal SAR Sentinel-1 for Camargue, France. *Remote Sens.* **10(8)** 1217

[24] Wang W, Dou D, Jiang Z and Sun L 2018 A fast dense spectral-spatial convolution network framework for hyperspectral images classification. *Remote Sens.* **10** 1068

[25] Yu L, Zhang M, Wang L, Qin W, Lu Y and Li J 2020 Clear-sky solar radiation changes over arid and semi-arid areas in China and their determining factors during 2001-2015. *Atmos. Environ.* **223** 117198

[26] Chen S and Billings S A 1992 Neural networks for nonlinear dynamic system modeling and identification. *Int. J. Control*. **56** 319

[27] LeRoux N and Bengio Y 2010 Deep belief networks are compact universal approximators. *Neural Comput.* **22** 2192

[28] Ghimire S, Deo R C, Raj N and Mi J 2019 Deep learning neural networks trained with MODIS satellite-derived predictors for long-term global solar radiation prediction. *Energies.* **12** 1

[29] Ghimire S, Deo R C, Raj N and Mi J 2019 Deep solar radiation forecasting with convolutional neural network and long short-term memory network algorithms. *Appl. Energy*. **253** 113541

[30] Ghimire S, Deo R C, Downs N J and Raj N 2019 Global solar radiation prediction by ANN integrated with European Centre for medium range weather forecast fields in solar rich cites of Queensland Australia. *J. Clean. Prod*. **216** 288

[31] Ciresan D, Meier U and Schmidhuber J 2012 Multi-column deep neural networks for image classification. *Proc. 2012 IEEE Conf. Computer Vision and Pattern Recognition*. 3642

[32] Kruger N, Janssen P, Kalkan S, Lappe M, Leonardis A, Piater J and Rodriguez-Sanchez AJ, Wiskott L 2013 Deep hierarchies in the primate visual cortex: What can we learn for computer vision? *IEEE Trans. Pattern Anal. Machine Intel*. **35(8)** 1847

[33] Qi Y, Karimian H and Liu D 2019 A hybrid model for spatiotemporal forecasting of PM2.5 based on graph convolutional neural network and long short-term

memory. *Sci. Total Environ.* **664** 1

[34] Zhu X X, Tuia D, Mou L, Xia G-S, Zhang L, Xu F and Fraundorfer F 2017 Deep learning in remote sensing: A comprehensive review and list of resources. *IEEE Geosci. Remote Sens. Mag.* **5(4)** 8

[35] Hinton G and Osindero S 2006 The YW. A fast learning algorithm for deep belief nets. *Neural Comput.* **18(7)** 1527

[36] Hinton G, Srivastava N, Krizhevsky A, Sutsever I and Salakhudinov R R 2012 Improving neural networks by preventing co-adaptation of feature detectors. arXiv:1207.0280

[37] Nair V and Hinton G 2010 Rectified linear units improve restricted Boltzmann Machines. *Proc. 27th Int. Conf. Mach. Learn.* 807

[38] Peel M C, Finlayson B L and McMahon T A 2007 Updated world map of the Köppen-Geiger climate classification. *Hydrol. Earth Syst. Sci.* 11 1633

[39] Korea Meteorological Agency 2009 Development of meteorological data processing system for communication, ocean and meteorological satellite (ATBD). Seoul

[40] Kim H, Lee KS, Seo M, Choi S, Sung NH, Lee D, Jin D, Kwon C, Huh M and Han KS 2016 The sensitivity analysis to observed frequency of daily composite insolation based on COMS. *Korean J. Remote Sens.* **32(6)** 733 (English abstract included)

[41] Kawai Y and Kawamura H 2005 Validation and improvement of satellite-derived surface solar radiation over the northwestern Pacific Ocean. *J. Oceanogr.* **61** 79

[42] Kawamura H, Tanahashi S and Takahashi T 1998 Estimation of insolation over Pacific Ocean off the Sanriku Coast. *J. Oceanogr.* **54** 457

[43] Yeom J M, Han K-S and Kim J-J 2012 Evaluation on penetration rate of cloud for incoming solar radiation using geostationary satellite data. *Asia-Pacific J. Atmos. Sci.* **48** 115

[44] Yeom, J M, Seo Y, Kim D and Han K-S 2016 Solar radiation received by slopes using COMS imagery, a physically-based radiation model, and GLOBE. *J Sens.* 4834579

[45] Bengio Y, Simard P and Frasconi P 1994 Learning long-term dependencies with gradient descent is difficult. *IEEE Trans. Neural Network.* **5(2)** 157

[46] Hochreiter S, Bengio Y, Frasconi P and Schmidhuber J 2001 Gradient flow in recurrent nets: the difficulty of learning long-term dependencies *A field guide to dynamical recurrent networks* ed J F Kolen and S C Kremer(Wiley-IEEE Press) p. 237

[47] Fan J, Li Q, Hou J, Feng X, Karimian H and Lin S 2017 A spatiotemporal prediction framework for air pollution based on deep RNN. *ISPRS Annal. Photogram. Remote Sens. Spatial Inf. Sci.* **4** 15

[48] Gong C, Qi L, Heming L, Karimian H and Yuqin M 2017 Spatio-temporal simulation and analysis of regional ecological security based on LSTM. *ISPRS Annal. Photogram. Remote Sens. Spatial Inf. Sci.* **4** 153

[49] Shi X, Chen Z, Wang H and Yeung D Y 2015 Convolutional LSTM network: A machine learning approach for precipitation nowcasting. arXiv:1506.04214

[50] Paparaju T 2018 Video frame prediction with Keras, https://medium.com/machine-learning-basics/video-frame-prediction-with-keras-f74dd4743a1f [accessed

20th May 2019].

[51] Pearce T 2017 CIKM AnalytiCup 2017 challenge entry, https://github.com/TeaPearce/precipitation-prediction-convLSTM-keras/blob/master/README.md [accessed 20th May 2019].

[52] Ioffe S and Szegedy C 2015 Batch normalization: Accelerating deep network training by reducing internal covariate shift. arXiv:1502.03167

[53] He L, Zhang X, Ren S and Sun J 2015 Delving deep into rectifiers: Surpassing human-level performance on ImageNet classification. *Proc. IEEE Int. Conf. Comput. Vis.* 1026

[54] Glorot X and Bengio Y 2010 Understanding the difficulty of training deep feedforward neural networks. *Proc. 13th Int. Conf. Artif. Intell. Stat.* 249

[55] Yeom J M and Han K S 2010 Improved estimation of surface solar insolation using a neural network and MTSAT-1R data. *Comput. Geosci.* **36** 590

[56] Breiman L 2001 Random forests. *Mach Learn.* **4**

[57] Park S, Shin M, Im J, Song C K, Choi M, Kim J, Lee S., Park R, Kim J, Lee D-W and Kim S-K 2019 Estimation of ground-level particulate matter concentrations through the synergistic use of satellite observations and process-based models over South Korea. *Atmos Chem Phys.* **19** 1097

[58] Cook D. 2016 Practical machine learning with H2O. Sebastopol, CA, USA O'Reilly

[59] Qin W, Wang, L, Lin A, Zhang M, Xia X, Hu B and Niu Z 2018 Comparison of deterministic and data-driven models for solar radiation estimation in China. *Renew. Sustain. Energy Rev.* **81** 579